LA-7939-MS
Informal Report

Irradiation Damage in Metals Produced by 800-MeV Protons

University of California
LOS ALAMOS SCIENTIFIC LABORATORY
Post Office Box 1663 Los Alamos, New Mexico 87545

LA-7939-MS
Informal Report

UC-25
Issued: July 1979

Irradiation Damage in Metals Produced by 800-MeV Protons

R. D. Brown
W. F. Sommer
W. V. Green

IRRADIATION DAMAGE IN METALS PRODUCED BY 800-MeV PROTONS

by

R. D. Brown, W. F. Sommer, and W. V. Green

ABSTRACT

Theoretical calculations of damage energies in metals from 800-MeV proton irradiation motivated an experimental transmission electron microscopy study of the damage produced. Damage produced by 800-MeV protons is accompanied by a higher level of helium production than for reactor neutron irradiation. To allow irradiation of samples on a routine basis, a proton irradiation port (PIP) was constructed in beam line A at LAMPF. This port allowed a high damage-rate irradiation of metal foils several mils thick. Irradiations were completed on foils of aluminum, niobium, molybdenum, and vanadium to damage levels between 0.05 dpa and several dpa, the damage occurring at homologous temperatures above 0.5 T_m.

Disks were punched from the irradiated foils and thinned for TEM examination. No voids were observed in irradiated aluminum samples. Molybdenum samples showed a low density of cavities which were believed to be gas filled at these high temperatures. Vanadium samples showed a high density of irradiation-produced defects resulting from irradiation-injected impurities. Such defects have been reported previously in ion-irradiated vanadium. The nature of the damage produced is compared to that found at lower temperatures following neutron or ion bombardment.

Introduction

Results of a theoretical study of the damage produced by 800-MeV protons in materials motivated an experimental study of this damage. It was known that protons in this energy range would interact with the target nuclei and spall off protons, neutrons and heavier particles. This would result in spallation products being created together with rather large quantities of hydrogen and helium, much of which would remain in a thick target. Coulter's[1] calculation for copper and later results for other materials developed the spallation product recoil spectrum shown in Fig. 1 for aluminum. The high recoil energies of many spallation products are important in producing damage in the target. When the damage energy contributions from various products are computed and compared, the heavier products are found to have the greatest influence. Computation of the damage energy cross section indicated the high dpa rate which could be produced by such irradiation. Table I compares the rates of damage production from 800-MeV protons, the fast neutron spectrum of EBR II, and that expected for the UWMAK-I, a fusion reactor design. The proton range was much larger than the thickness of specimens required for mechanical property testing, allowing for a uniform damage distribution through such samples. Production of high damage levels was coincident with production of large amounts of

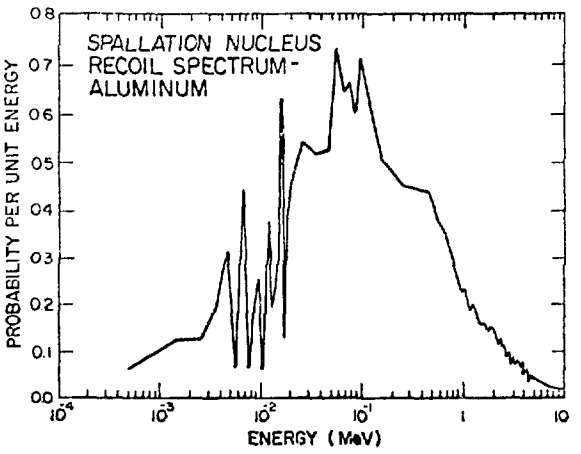

Fig. 1
The spallation product recoil spectrum is shown for 800-MeV protons on aluminum.

helium and hydrogen. This suggested possible accelerated testing of materials in an environment of high helium production which is known to enhance void nucleation.[2] Measurements of the proton cross sections for spallation product formation had been made by the nuclear chemistry group at Los Alamos,[3,4] and aided in confirming the accuracy of the calculations.

The combination of long proton range in metals together with the high displacement rate predicted by the theoretical study suggested that scoping irradiations be performed to ascertain the nature of the damage produced in several metals. In addition to high Z-spallation products, the importance of helium production and its retention in targets to void nucleation and growth required that helium concentration measurements be made.

Experimental Procedure

To allow 800-MeV proton irradiation on a routine basis, a location was chosen in the LAMPF beam line where high dpa rates could be achieved and a proton irradiation port (PIP) was constructed. The PIP provided a suitable stringer together with the necessary cooling and electrical feedthroughs for routine irradiations. Figure 2 shows an early view from outside the beam line A shield wall. The proton beam at PIP is Gaussian in profile, with typical two sigma values of 2.5 mm horizontal and 1 mm vertical. At the onset of experimental work, the total beam current was 100 μA, resulting in a current density of about 8 A/m^2. This resulted in specimen heating, but the effect was tolerable. Subsequent increases in the beam line A current led to melting of aluminum specimens. Temperature calculations indicate that for present beam currents at PIP, specimens must be kept thin even when immersed in cooling water to avoid severe internal temperature gradients. A second factor limiting the thickness of specimens at the present PIP facility is the scattering of the proton beam to experimenters downstream. At present this has limited aluminum samples to a thickness of 0.25 mm.

TABLE I.

REACTION RATES FOR HIGH ENERGY PROTONS, EBR-II, AND UWMAK-I IN ALUMINUM

Facility	Displacements dpa/sec	Helium appm Helium/dpa	Hydrogen appm Hydrogen/dpa
LAMPF[a]	$7. \times 10^{-6}$	70.	520.
EBR-II[b]	4.2×10^{-6}	0.12	0.6
UWMAK-I, First Wall[c]	0.9×10^{-6}	15.	12.

[a]800-Mev Protons at 10 A/m^2 (this experiment).
[b]$\phi_T = 2.7 \times 10^{15}$ n/cm^2 s.
[c]$\phi_T = 4.7 \times 10^{14}$ n/cm^2 s.

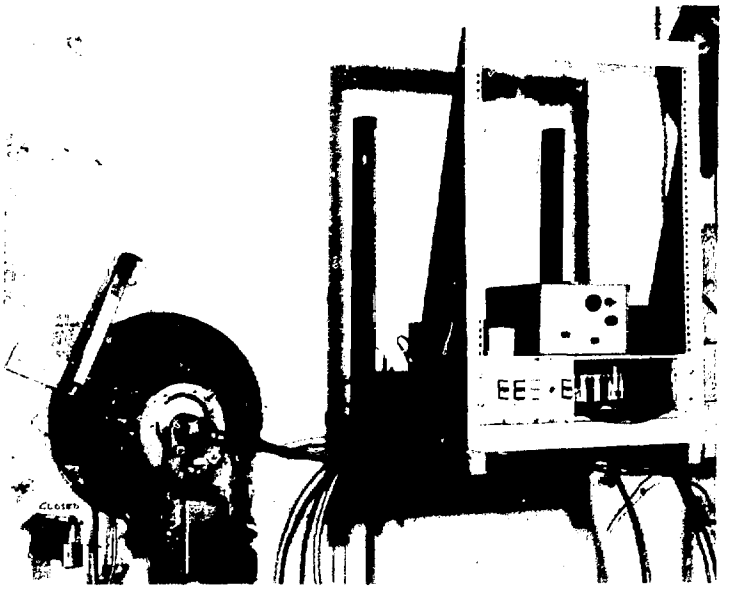

Fig. 2.
The proton irradiation port is viewed from outside the beam line A shield wall. The relay rack at right houses the controls which position the stringer. Cooling lines and a conduit for electrical feedthroughs are provided in the stringer.

With the construction of the proton irradiation port at LAMPF, a program of 800-MeV proton irradiation of several metals was started. The damage produced by such high energy protons in metals had never been previously studied. It was decided to evaluate the results of these experiments using transmission electron microscopy to facilitate comparisons with damage produced by other types of radiation at comparable fluences and temperatures. An fcc metal, aluminum, was chosen because damage produced by a variety of other particles at various fluences and temperatures had been well characterized. Three bcc metals were evaluated. Molybdenum has been well studied and is not a hydride former, while vanadium and niobium are. This allowed an examination to be made of the effects of high hydrogen production levels on the microstructure of hydride formers. Several of these materials are of interest due to their low swelling during neutron irradiation where little helium or hydrogen is formed.

Actual irradiations were begun on aluminum strips in May 1977, and a second set of five aluminum samples was irradiated to between 1 and 5 dpa later that month. Near the end of this run the proton current density increased to approximately 18 and then to 32 A/m^2. Such high current densities led to melting of the specimens and it was decided to begin work on the higher melting point bcc metals. The third run involved vanadium, niobium and molybdenum samples which were irradiated to between 2 and 16 dpa. A fourth run involved irradiation of five molybdenum samples to 3 dpa, and the fifth run, irradiation of molybdenum and vanadium to 0.2 and 25 dpa.

Understanding the nature of the damage following irradiation required that the proton fluence and irradiation temperature be known. The maximum fluence was calculated from the beam current as measured by current monitors together with the beam size as determined from the harps. To determine the fluence at the areas thinned for TEM examinations, the individual samples were autoradiographed before punching TEM disks. Individual disks were autoradiographed following punching and then thinned for TEM observation. A comparison of the intensity in the area where perforation occurred with that of the sample prior to

punching the disks allowed a reasonable estimate of the relative fluence in the thinned region to be made.

Temperatures were experimentally checked by spot welding thermocouples to the samples. Thermocouples struck by the beam were melted, so that only temperatures outside the central beam area could be monitored. To obtain a better temperature profile a computer calculation was used in which heat was supplied to a thin disk. The heat was applied with a Gaussian spatial distribution and a pulsed time structure defined by the LAMPF beam. The rim of the disk was maintained at 300 K, heat being removed by conduction to the rim and radiation from the surfaces. Because of the high temperatures encountered in the beam-heated area, temperature-dependent values of the thermal conductivity, thermal diffusivity and emissivity[5] were used. Figure 3 compares the calculated temperature distribution with that found experimentally using thermocouples for a molybdenum sample. To allow some comparison between the 800-MeV proton irradiation results and neutron irradiation results, Fig. 4(a)-(c) plots the percentage of swelling for the three materials examined as a function of fluence (converted to dpa) and homologous temperature. It can be seen that our 800-MeV proton irradiations were made at very high temperatures, well above the peak swelling range. The fluences listed are the values for the actual regions examined in the electron microscope.

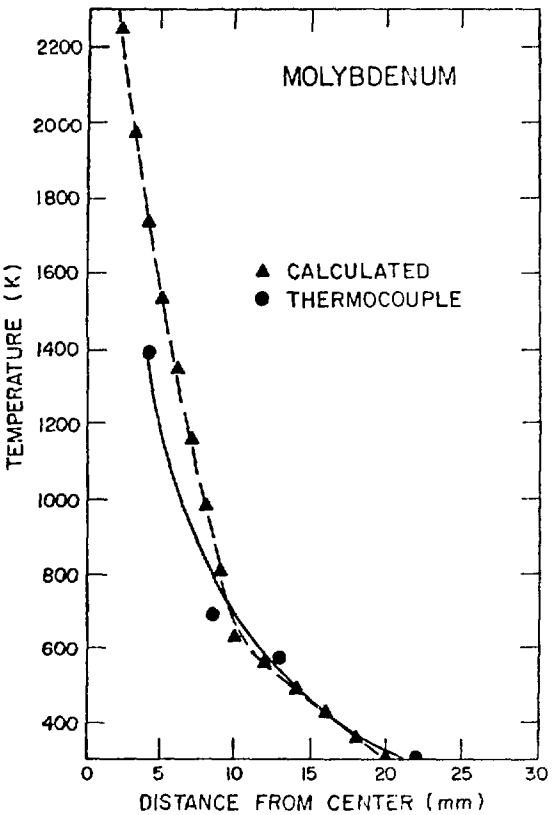

Fig. 3.
The temperature distribution measured by thermocouples is compared to the calculated temperature distribution for a molybdenum sample. Beam size and current were based on LAMPF measurements.

Results

Initial examination of the irradiated samples was through study of the photomacrographs taken following irradiation. This reduced considerably the radiation exposure from the samples, several of the sample holders registering about 100 R/hr on contact. The melting of holes in the aluminum samples was easily verified from these photographs (see Fig. 5). A specimen irradiated at 8 A/m^2 to 22 dpa [see Fig. 6(a)] was embrittled along the grain boundaries. The scanning electron microscope confirmed the presence of deep grain boundary cracks in this specimen [see Fig. 6(b)]. This suggested either embrittlement due to the relatively poor vacuum and high temperature, or the segregation of spallation products to the grain boundaries.

Disks were punched from several irradiated aluminum foils for thinning and TEM examination. Attempts at electropolishing disks from the highest fluence regions proved futile due to preferential penetration through the grain boundaries. Disks punched from areas irradiated to a few tenths of a dpa could be successfully thinned and were examined.

All of the irradiated samples examined showed a dislocation density of the order of 10^{13}/m^2 as shown in Fig. 7. Figure 8 indicates the dislocation density to be very similar in unirradiated areas of the specimen. Figures 7 and 8 show that black circular defects are present in the irradiated areas but not in

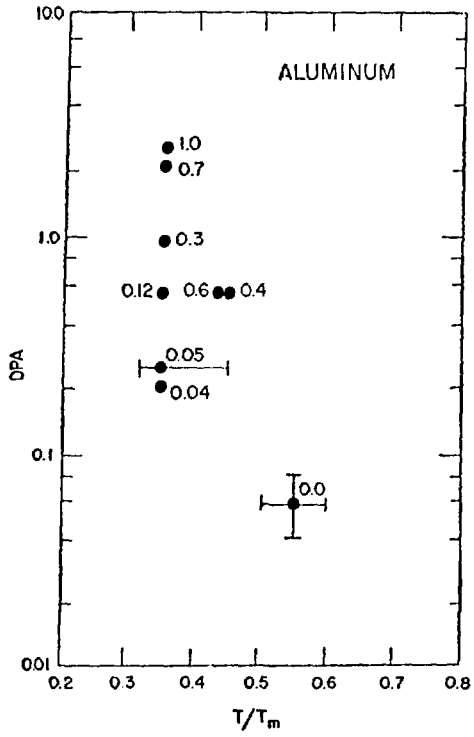

Fig. 4(a).

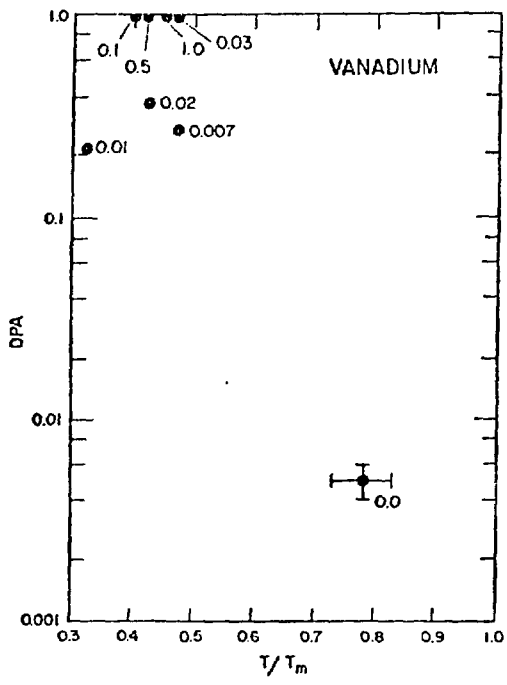

Fig. 4(c).

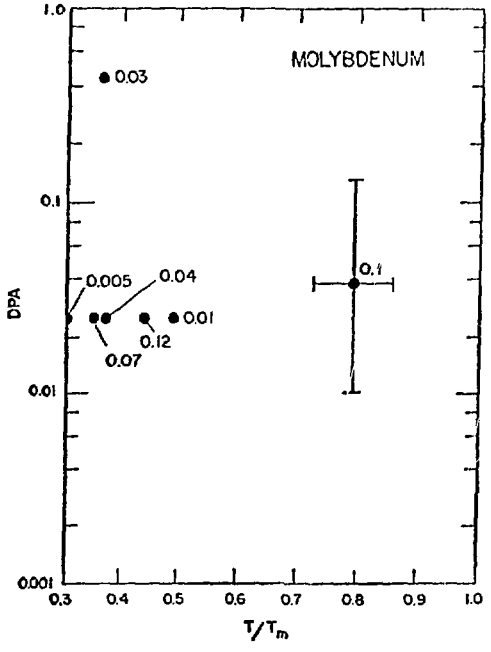

Fig. 4(b).

Fig. 4(a)-(c).
The points indicate the fluence in dpa and the homologous temperature for samples irradiated under various conditions. The numbers indicate the observed percentage of swelling. Except for the point labeled 800-MeV proton irradiation, the other points apply to neutron irradiations with the dpa values being computed from the neutron fluences for which $E > 0.1$ Mev.

Fig. 5.
The sample holder is shown following proton irradiation of aluminum samples. The proton current density was 18 A/m². Note the melting which has occurred.

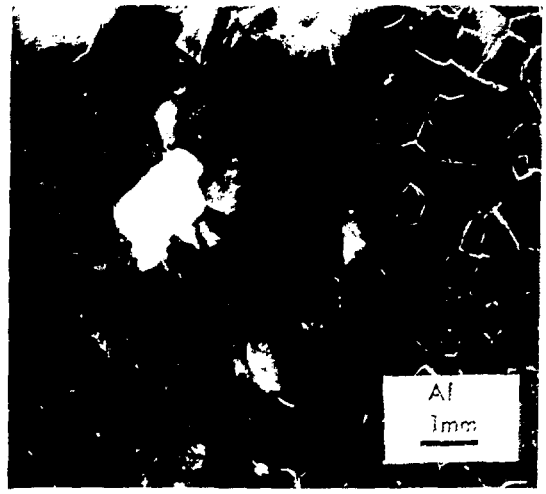

Fig. 6(a).
An aluminum foil is shown after irradiation to 22 dpa at a proton current density of 8.4 A/m². The grain boundaries are clearly delineated, and one or more grains have been broken out of the irradiated area.

the unirradiated areas. From a more detailed study of these defects imaged under a series of diffraction conditions in dark field, they are clearly not loops, many of which are visible and show the characteristic double arc contrast. High angle tilting results in little change in measured defect diameter, indicating the defects are nearly spherical. The dark field images always show these defects to be darker than the background, as is true in bright field. They do not show observable Fresnel fringes, as do voids, nor any strong strain contrast as might be expected around precipitates. If these defects are precipitates, they cannot be formed entirely from spallation products, as the defects are about 70 volume ppm, while no more than 5 volume ppm of spallation products are calculated to be generated. This would imply that the precipitates depend on impurities injected into the foils during irradiation.

Disks have been thinned for TEM observation from several of the molybdenum samples. Figure 9(a) and (b) illustrates that bubbles are formed in the molybdenum samples during irradiation at temperatures between 0.72 and 0.86 T_m. The bubbles are present at very low density and are heterogeneously distributed along dislocation lines. No other defect structure is visible in these samples, strongly suggesting that the high temperature has

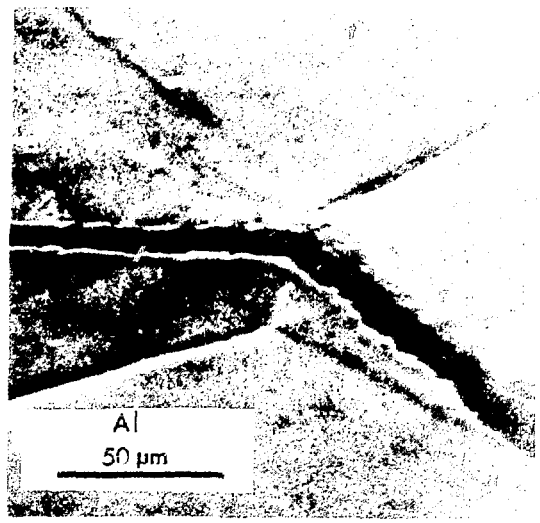

Fig. 6(b).
A grain boundary crack is shown from the surface of the same sample in Figure 6(a). This crack extends into the foil from the hole observed in Fig. 6(a).

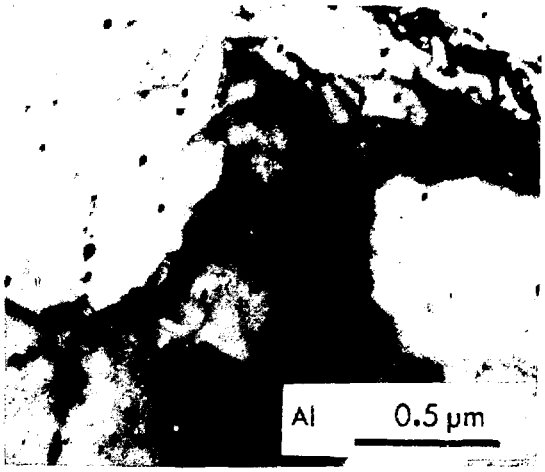

Fig. 7(a).
Transmission electron micrographs are shown for the damage in an aluminum specimen irradiated to approximately 0.05 dpa.

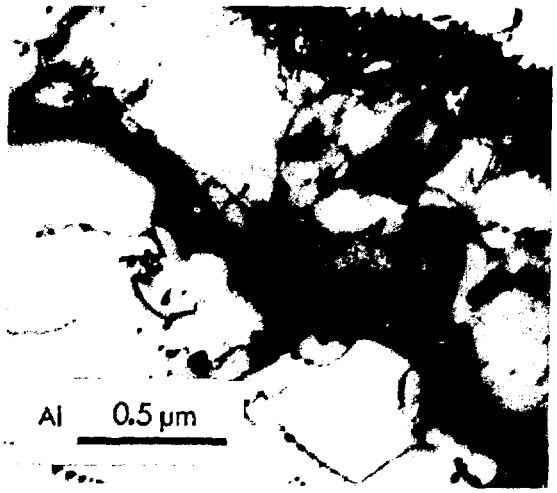

Fig. 8.
An unirradiated area from an aluminum specimen has a dislocation density of $2.4 \times 10^{13}/m^2$. A few dislocation loops are present, but the black dot contrast present in the irradiated areas is absent.

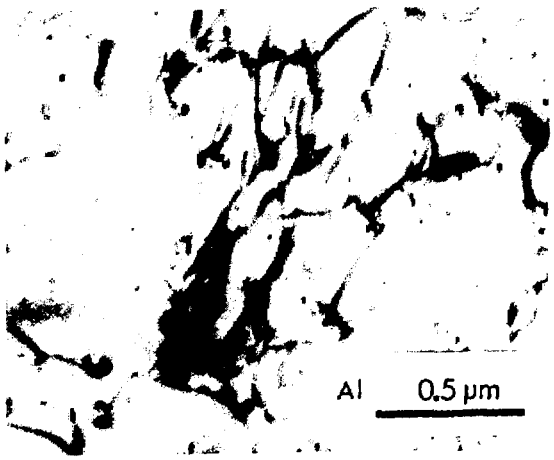

Fig. 7(b).
This micrograph shows another area from the same specimen as in Fig. 7(a), irradiated to 0.08 dpa. The dislocation density is $2.2 \times 10^{13}/m^2$, typical of most of the areas examined. Black dot contrast is present in both areas of the sample.

annealed out any other defects produced. An unirradiated area from the same specimen is shown in Fig. 10. As expected, bubbles are not found in this area. No precipitates are present.

The photomacrographs showed that a vanadium sample irradiated to 0.5 dpa was in two pieces. Tests on samples of vanadium resistively heated in a 3 μm vacuum showed that severe embrittlement occurred within several minutes, suggesting that contamination of the material from the vacuum followed by stressing could account for the fractures. The vanadium sample, however, had clearly been melted by the beam as shown in Fig. 11. A second vanadium sample, irradiated when the beam was larger and the current density lower by a factor of 2.8, did not melt. This is in agreement with the observation that only a region about 0.5 mm wide was melted in the first sample.

TEM examination of the vanadium samples revealed a high density of defects, as shown in Fig. 12. Two forms of defect were apparent. A high density of small (50 Å to 400 Å) loop-type defects was present throughout the foil (see Fig. 13). A lower density of planar defects was present, with the loop-type defects denuded in regions near the planar

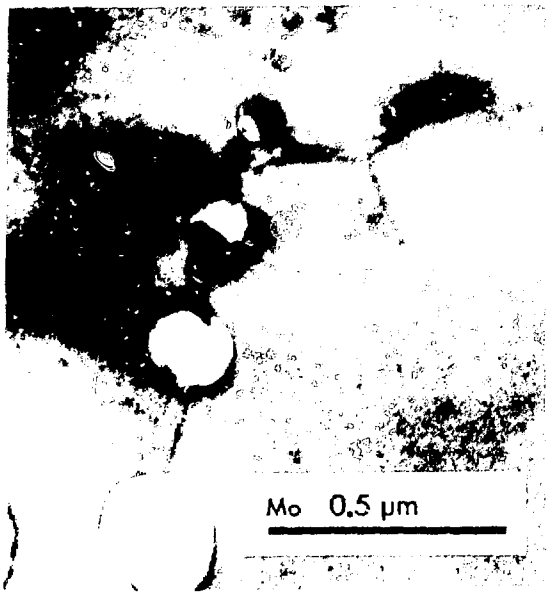

Fig. 9(a).
The defect structure created in a molybdenum foil following irradiation to ~.05 dpa between 0.72 T_m and 0.86 T_m is shown. The bubbles are connected by dislocations and their distribution is very heterogeneous.

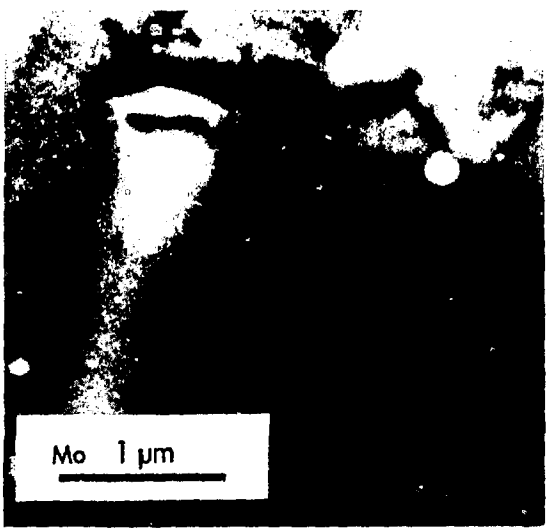

Fig. 9(b).
An adjoining area illustrates the heterogeneity of the bubble distribution.

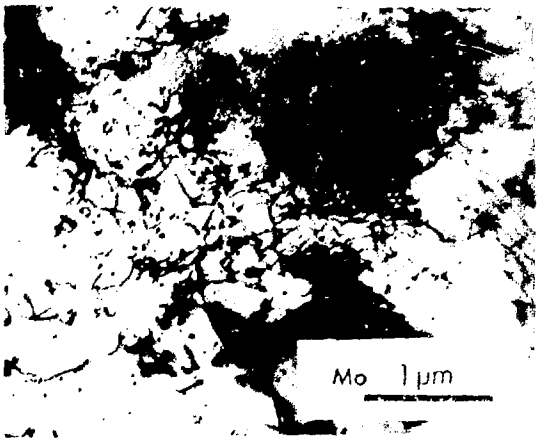

Fig. 10.
An unirradiated area from the same molybdenum specimen as in Fig. 9 is shown.

defects (see Fig. 14). Dark field imaging of the smaller defects shows strain field contrast. It is not certain whether these were loops or small precipitates, but the presence of the large precipitates surrounded by a denuded zone suggests them to be small precipitates. This would suggest that the large precipitates might form from a high density of the smaller ones. It is likely that these defects were created from impurities injected into the foil. Many observations have been made of such defects in vanadium,[6-9] with the exact precipitate nature depending on the details of the surface preparation and irradiation. An area of unirradiated vanadium from the same specimen shown in Fig. 15 indicates that the grain size is much smaller and no defect structure is in evidence. The large grain size in the irradiated area is due to annealing of the sample by beam heating.

Discussion

As indicated by Fig. 4(a)-(c), all of the samples were irradiated at temperatures well above that for peak swelling. The molybdenum sample received a high enough fluence that even at a temperature far in excess of the peak swelling temperature, some bubbles were present. Their presence along segments of dislocation line suggests that the dislocation lines may have acted as nucleation centers for

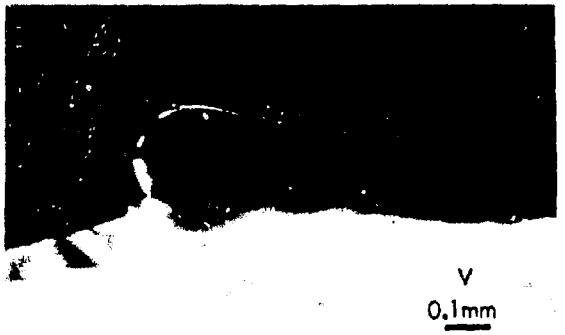

Fig. 11.
The edge of a melted vanadium sample is shown. The region to the left fractured brittlely during handling.

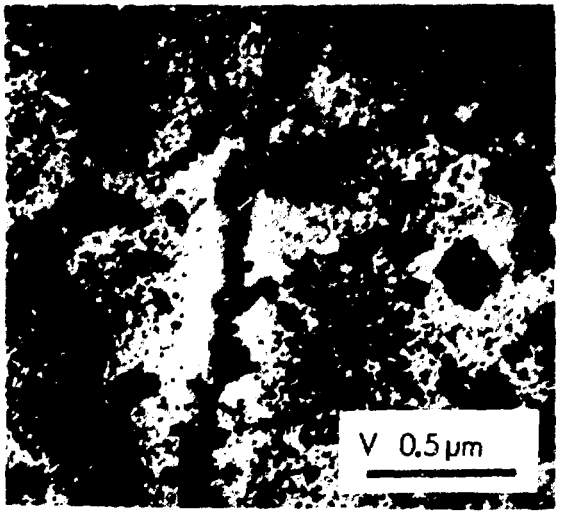

Fig. 13.
A detailed view of defects formed in vanadium. The small loop-like defects are denuded around the larger planar defects. These planar defects often exhibit stacking fault fringe contrast.

the bubbles. A rough calculation of the amount of helium produced during irradiation suggests that enough was available to maintain the bubbles against shrinkage caused by surface tension. The swelling is low as compared [Fig. 4(b)] with previous studies of neutron-irradiated molybdenum samples.

In the cases of aluminum and vanadium, the combination of low fluences and high temperatures has resulted in no detectable swelling in the specimens examined. For the aluminum, only a low density of radiation-produced defects was observed and these are most likely due to impurities introduced during irradiation. This was also the case for the vanadium, in which this irradiation-introduced precipitation has been observed previously.

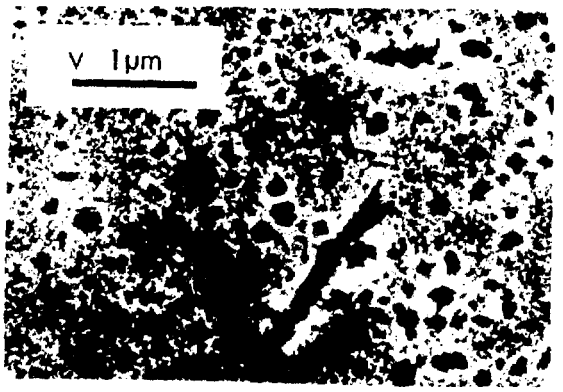

Fig. 12.
A transmission electron micrograph of vanadium irradiated to ~0.1 dpa illustrates the defects formed.

Clearly these initial scoping runs must be repeated over a lower temperature range to obtain data more useful to fusion reactor materials. Irradiations now planned will utilize the lower beam current and larger beam size in experimental line B to greatly reduce the specimen heat load. Heating calculations are now available which can predict specimen temperatures in three dimensions for given beam parameters and surface cooling. This allows a preliminary study of specimen temperature to be made so that thickness will not be so great as to result in overly large internal temperature gradients. In addition to temperature considerations, improved vacuum conditions will be required to prevent anomalous results in materials such as vanadium.

To aid in better understanding the results of 800 MeV proton irradiations, two experiments are being considered. The first involves the use of dislocation

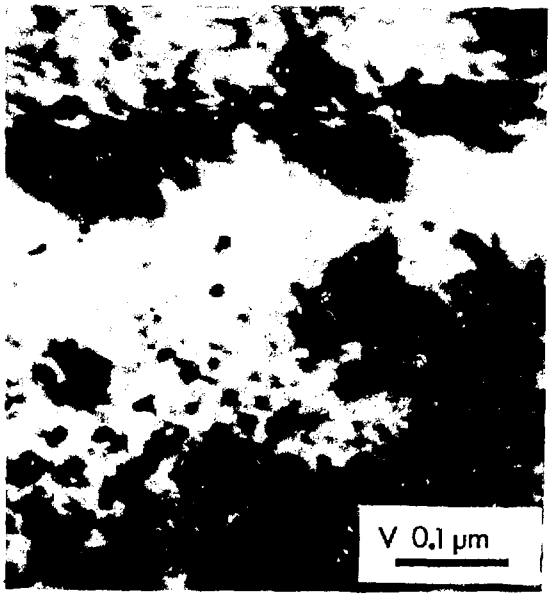

Fig. 14.
A high magnification view of the area shown in Fig. 13 shows a planar defect at the right. To the left, a high density of loop-like defects exists. The density of such small defects drops sharply as the planar defect is approached.

pinning experiments previously run for monoenergetic neutrons[10] to determine the number of interstitials which escape the cascades. A second experiment is now underway to test the hypothesis that dislocation vibration can reduce the extent of swelling in irradiated materials.[11]

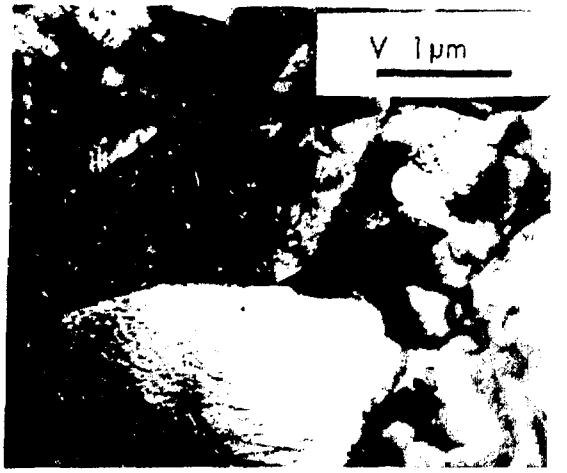

Fig. 15.
An unirradiated area of the sample shown in Figs. 12-14 shows no defect structure. The grain size is smaller, as there was no beam heating to allow grain growth.

REFERENCES

1. C. A. Coulter, D. M. Parkin, and W. V. Green, "Calculation of Radiation Damage Effects of 800-MeV Protons in a "Thin" Copper Target," J. Nucl. Mater. **67**, 140 (1977).

2. K. Farrell, A. Wolfenden, and R. T. King, "The Effects of Irradiation Temperature and Preinjected Gases on Voids in Aluminum," Radiat. Eff. 8, 107 (1971).

3. B. J. Dropesky and H. A. O'Brien, Jr., "Accelerator-Produced Radioisotope Program. Quarterly Report, July 1 — September 30, 1972," Los Alamos Scientific Laboratory report LA-5120-PR (1972).

4. B. R. Erdal *et al.*, *Nuclear Cross Sections and Technology*, p. 492, NBS Special Publication **425**, 1975.

5. Y. S. Touloukian *et al.*, *Thermophysical Properties of Matter* (IFI-Plenum, New York, 1973).

6. S. C. Agarwal and A. Taylor, "Dose Dependence of Void Swelling in Vanadium Irradiated with Self Ions," in *Radiation Effects and Tritium Technology for Fusion Reactors*, CONF-750989, Vol. I, p. 150 (1976).

7. W. J. Weber *et al.*, "Ion Simulation Study of Void Formation in High-Purity Vanadium," *ibid.*, Vol I, p. 130 (1976).

8. J. D. Elen, G. Harnburg, and A. Mastenbroek, "Voids in Vanadium, Niobium, and Molybdenum by Fast Neutron Irradiation at High Temperatures," J. Nucl. Mater. **39**, 194 (1971).

9. M. Cambini, J. Bressers, and M. Heerschap, "Void Swelling Upon Neutron Irradiation in Helium Preinjected Vanadium," J. Nucl. Mater. **62**, 311 (1976).

10. J. Roberts Goldstone, "A Comparison of Initial Damage Rates Using Neutron and Electron Irradiation," Thesis, State University of New York at Stony Brook, 1978.

11. W. V. Green and J. Weertman, "Increased Efficiency of a Dislocation Line as a Sink for Vacancies When It Oscillates," Radiat. Eff. **22**, 9 (1974).